q_1 Charge-Density Wave in $NbSe_3$

A. H. Moudden,[1],[a] J. D. Axe,[2] P. Monceau,[3] and F. Levy[4]

[1]*Laboratoire Léon Brillouin, Commissariat à l'Energie Atomique-Centre National de la Recherche Scientifique, Centre d'Etudes Nucléaires de Saclay, F-91191 Gif-sur-Yvette, France*

[2]*Physics Department, Brookhaven National Laboratory, Upton, New York 11973*

[3]*Centre de Recherche sur les Très Basses Températures, Centre National de la Recherche Scientifique, BP 166X, F-38042 Grenoble CEDEX, France*

[4]*Institut de Physique Appliquée, Ecole Polytechnique Fédérale, CH-1015 Lausanne, Switzerland*

(Received 29 January 1990)

Using synchrotron x-ray measurements on $NbSe_3$, we show that the scattering associated with the q_1 charge density wave (CDW) reflects a 2D regime of fluctuations with in-plane anisotropy $\xi_b*/\xi_a* = 3.5 \pm 0.5$. The plane of 2D fluctuations is likely to be formed by the chains with the shortest Se-Se pairing. 3D coupling sets in within 2 K above the transition temperature $T_1 \approx 150$ K with out-of-plane anisotropy $\xi_b*/\xi_c* = 27 \pm 2$. q_1 has a significant variation from 0.2445(1) at T_1 to 0.2411(1) at ≈ 80 K and then remains constant to the lowest temperatures. Upon cooling, q_1 is driven far away from $\frac{1}{4}$. No anomaly in either the amplitude or phase of q_1 is observed at the q_2-CDW transition.

PACS numbers: 71.45.Lr, 61.10.Lx, 64.70.Rh

$NbSe_3$ is known as a linear-chain compound which exhibits a variety of nonlinear transport properties associated with two moving charge-density waves[1] (CDW's) which are formed independently. The first one develops below $T_1 \sim 150$ K with a wave vector $\mathbf{q}_1 = (0,q_1,0)$, and the second one emerges below $T_2 \sim 60$ K with the wave vector $\mathbf{q}_2 = (0.5,q_2,0.5)$ referring to the $P2_1/m$ monoclinic symmetry of the undistorted room-temperature phase. Since the early electron-diffraction studies by Tsutsumi *et al.*,[2] who have shown the existence, above T_1, of diffuse scattering on a (b^*,c^*) photograph at the satellite position, and have interpreted it as diffuse sheets resulting from a Kohn anomaly, $NbSe_3$ has been considered as a quasi-one-dimensional system. The one dimensionality received strong support for the chainlike crystal structure and its fibrous morphology. However, using x-ray scattering, Fleming, Moncton, and McWhan[3] have shown that the anisotropy deduced from the measured correlation length ξ_b* parallel to the chains and ξ_a* perpendicular to the cleavage planes is about 5, and is not sufficient to consider a significant one dimensionality in $NbSe_3$. From dc measurements of transverse resistivity, Ong and Brill[4] have also found that the anisotropy is several orders of magnitude smaller than that of the standard 1D conductors. Further x-ray and electron-diffraction studies by Hodeau *et al.*[5] did not show any evidence of diffuse streaks and the authors concluded from the structural analysis of the bond lengths that $NbSe_3$ must be a 2D system in the cleavage (b,c) planes.

Using accurate synchrotron x-ray studies of the diffuse scattering, we will show that $NbSe_3$ exhibits a pronounced regime of 2D CDW fluctuations associated with the upper transition. We will show that the diffuse scattering observed by Tsutsumi *et al.*[2] are not streaks but are rods parallel to c^* that Fleming, Moncton, and McWhan[3] scanned transversely, revealing a modest anisotropy $\xi_b*/\xi_a* \approx 5$, and which we will show correspond to the anisotropy of the 2D correlations. We will also show that the planes of the 2D fluctuations of the q_1 CDW are not the cleavage planes (b,c) as suggested by Hodeau *et al.*[5] but are parallel to the (a,b) planes and are very likely to be the planes connecting the $NbSe_3$ chains with the shortest Se-Se pairing. We will report on the temperature evolution of the 2D correlation lengths as well as the crossover to the 3D regime of fluctuations and the development of the long-range order. We will show the existence of a substantial temperature dependence of the incommensurate wave vector q_1 mainly near the 3D ordering temperature T_1, while it tends toward a constant value at low temperature when the precursors of the second CDW start to develop.

The synchrotron x-ray-scattering studies were carried out on the X22C beam line at the National Synchrotron Light Source at Brookhaven National Laboratory. For high-momentum-transfer-resolution studies, we used 1.7-Å x rays from a Ge(111) double monochromator; a perfect Ge(111) analyzer was used as well. A single crystal of $NbSe_3$, about 5 by 0.2 mm along b and c, respectively, and much thinner along a^*, was mounted on a copper plate and glued by a small droplet of silver paint at one end of the crystal to avoid stresses on the sample from differential thermal contractions. The lattice parameters we measured at room temperature are consistent with those given in Ref. 5: $a = 10.009$ Å, $b = 3.480$ Å, $c = 15.629$ Å, and $\beta = 109.47°$.

In Fig. 1(a) we show two scans through the satellite position $(0,1+q_1,0)$ along the chain direction b^*, one at 80 K when the linewidth is resolution limited indicating a long-range order of the CDW with $\xi_b* > 2800$ Å, and the second at 155 K when the linewidth is larger than the instrumental resolution indicating a short-range-ordered CDW with $\xi_b* \sim 700$ Å. The solid lines represent a fit of the experimental data by a standard

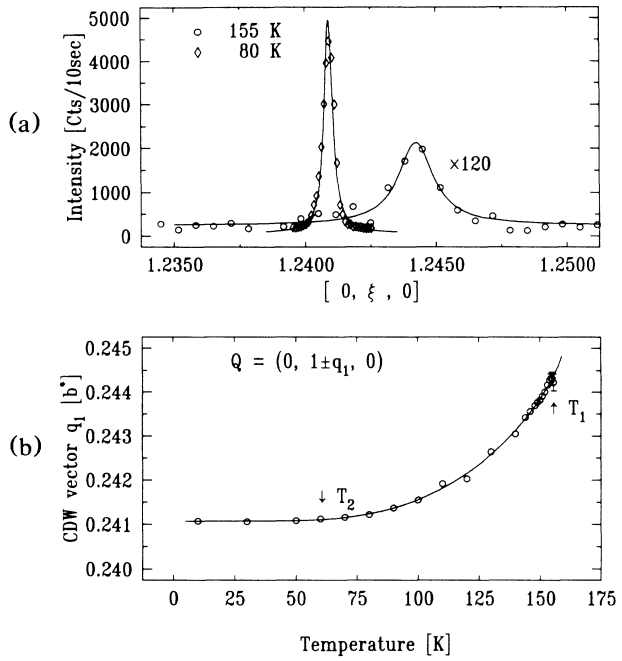

FIG. 1. (a) Longitudinal scan through the satellite reflection $(0,1+q_1,0)$ at 80 K compared to the same scan at 155 K through the diffuse scattering observed above the ordering temperature $T_1 \approx 150$ K. The solid lines are fits with Lorentzian profiles. (b) Temperature variation of the incommensurate component q_1 of the distortion wave vector. The solid line is a fit by an activated variation (see text).

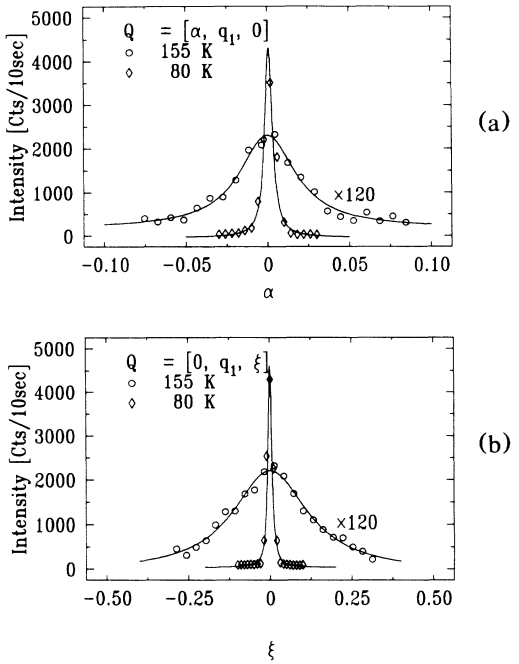

FIG. 2. Transverse scans through the satellite position $(0,1+q_1,0)$ above and below T_1 (a) along a^* and (b) along c^*.

Lorentzian line shape. Upon cooling, the scattering peak becomes narrower, increases in intensity, and shifts in position from about 0.2445(1) at T_1 to 0.2411(1) in units of b^* which was adjusted at each temperature to take into account the thermal expansion of the lattice. In Fig. 1(b) we show the temperature dependence of the incommensurate component q_1. Clearly one can see that most of the variation of $q_1(T)$ occurs between 150 and about 80 K, below which $q_1(T)$ remains constant at 0.2411(1). Notice that upon cooling the wave vector is driven far away from the simple commensurate value of $\frac{1}{4}$. Whether $q_1(T)$ locks into another commensurate number is yet to be understood. From our data the simple rational number we get for the best approximant to the low-temperature value of q_1 is $\frac{7}{29}$ which is a quite large commensurability order for a continuum modeling of an incommensurate-commensurate transformation. However, in Wilson's[6] picture of bonding involving every second pair of Nb atoms along the chains with the shortest Se-Se pairing, this ratio $\frac{7}{29}$ suggests one missing bond every seven periods which is not unreasonable. But when using this picture to understand qualitatively the temperature evolution of the wave number, a steplike variation is expected[6] for $q_1(T)$, since it should reflect a quantized variation of the number of bonds per chain determined by electron counting. Although our measured variation of $q_1(T)$ does not reveal such a behavior, the steps might be too small to be detected with our resolution. In fact, as shown by the solid line in Fig. 1(b), the global change of $q_1(t)$ is well accounted for by an activated variation of the form $q_1(T)=q_1(0)+C \times e^{-(\Delta E/T)}$, where C is a constant. The activation energy $\Delta E \approx 700$ K is surprisingly close to that reported for blue bronzes[7] and interpreted as due to a specific electronic band structure of the blue bronzes. Although we do not have yet a precise microscopic mechanism for this activated variation of the wave number, we feel that this is a new common feature to understand in these CDW systems.

In Fig. 2, we show transverse scans along a^* and along c^*, through the satellite position $(0,1+q_1,0)$ above and below T_1. The instrumental resolutions measured at 80 K along a^* and c^* are respectively 0.0018 and 0.0029 Å^{-1}, as a half width at half maximum of the satellite Bragg peak. Even though the resolution is somewhat better along a^* than it is along c^*, it is clear from the scales of the scans at 155 K that the diffuse scattering is an order of magnitude more elongated along c^* than it is along a^* and b^*, indicating quasi-two-dimensional fluctuations in the (a,b) planes. (We have measured $T_1 \approx 153.5$ K from the broadening of the satellite peaks; there might be 3-K difference between the sensor and the sample.) After a proper deconvolution of the scattering profile with the instrumental resolution is made at T_1+6 K, we obtain $\xi_{a^*} \approx 42$ Å and $\xi_{b^*} \approx 140$ Å, which are larger than the lattice parameters a and b,

whereas $\xi_{c^*} \approx 5$ Å is much smaller than the spacing c. When the details of the structure[5] are considered with the possibilities of interchain linkage of the three types of pairs of chains (termed[6] yellow, orange, and red for short, medium, and large Se-Se bonding, respectively), one can clearly see that while the orange and red chains are alternating with each other, the yellow chains define homogeneous slabs precisely parallel to the (a,b) planes of the 2D fluctuations associated with the q_1 CDW. Thus our observation provides strong support to the idea[6,8] that the yellow chains are involved in the upper transition.

We have measured the temperature dependence of the scattering profile along the three directions of the reciprocal lattice. The result for the inverse correlation lengths corrected for the instrumental resolution function is shown in Fig. 3. The solid lines are a parametrization with a power-law behavior of the form $\xi^{-1} \sim (T - T_1)^{\nu}$, with the exponent $\nu \sim 0.6$ for the three correlation lengths. We find for the in-plane anisotropy $\xi_{b^*}/\xi_{a^*} = 3.5 \pm 0.5$ and for the out-of-plane anisotropy $\xi_{b^*}/\xi_{c^*} = 27.0 \pm 2$. In Fig. 4 we show the temperature variation of the maximum intensity $I_D^{\max}$ at the critical wave vector. From the measured anisotropies it is clear that $NbSe_3$ is quasi-2D, and it is appropriate to analyze the observed CDW fluctuations in terms of weakly coupled layers using a more accurate approach of mean-field treatment of the 3D coupling assuming exact modeling for these CDW fluctuations in 2D.

Following Scalapino, Imry, and Pincus[9] we write the functional free energy as

$$F = \int\int dx\, dy \sum_i [a\Delta_i^2 + b\Delta_i^4 + c(\partial\Delta_i)^2] - \sum_{i \neq j} \lambda_{ij}\Delta_i\Delta_j , \quad (1)$$

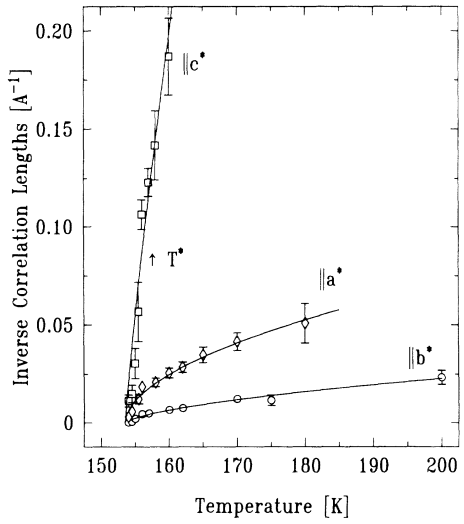

FIG. 3. Temperature dependence of the three 3D inverse correlation lengths obtained after deconvolution with the instrumental resolution. The solid lines are fits by power laws $(T - T_1)^{\nu}$.

where $\Delta_i(x,y)$ is a complex order parameter which describes the CDW in the ith plane and λ_{ij} is the interlayer coupling restricted to nearest-neighbor planes ($\lambda_{ii+1} = \lambda$); a, b, and c are constants which can be derived from the microscopic model of the CDW formation in 2D. At this level we consider a 2D susceptibility χ_{2D} associated with the order parameter Δ as given by

$$\chi_{2D}^{-1}(q) = \chi_{2D}^{-1}(0)[1 + \xi_{2D,x}^2 q_x^2 + \xi_{2D,y}^2 q_y^2]^{1-\eta/2} , \quad (2)$$

where $\xi_{2D,x}$ and $\xi_{2D,y}$ are the correlation lengths along x and y and η is the appropriate exponent in 2D. The mean-field treatment of the 3D coupling leads to

$$\chi_{3D}^{-1}(q) = \chi_{2D}^{-1}(q_x,q_y) - 2\lambda\cos(q_z d_\perp) , \quad (3)$$

where $d_\perp$ is the interlayer spacing and $\chi_{3D}(q)$ is the static 3D susceptibility which we determine experimentally from the diffuse scattering $I_D(q)$ according to the fluctuation-dissipation theorem which, in the temperature range of interest, applies in its classical form, $I_D(q) \sim S(q) = kT\chi_{3D}(q)$. Identifying the 3D ordering temperature T_1 as the temperature at which $\chi_{2D}^{-1} = 2\lambda$ and expanding Eq. (3) around the critical wave vector leads to the 3D correlation lengths given by

$$\xi_{3D,j}^2 \approx \xi_{2D,j}^2(1 - 2\lambda\chi_{2D}), \quad j = x,y , \quad (4)$$

$$\xi_{3D,z}^2 \approx d_\perp^2 \lambda\chi_{2D}/(1 - 2\lambda\chi_{2D}) . \quad (5)$$

Using Eqs. (4) and (5) and the measured 3D anisotropy we get $\xi_{2D,y}(T = T_1) = 406 \pm 30$ Å and $\xi_{2D,y}/\xi_{2D,x} = 3.5 \pm 0.5$. Defining T^* as the temperature at which the 3D correlation $\xi_{3D,z}(T^*)$ equals the interlayer spacing $d_\perp$ leads to the coupling constant $\lambda = \chi_{3D}^{-1}(T^*)$ which can be determined numerically from our experiments if a proper normalization of the diffuse scattering intensity is made. Making use of the satellite Bragg intensity I_B measured

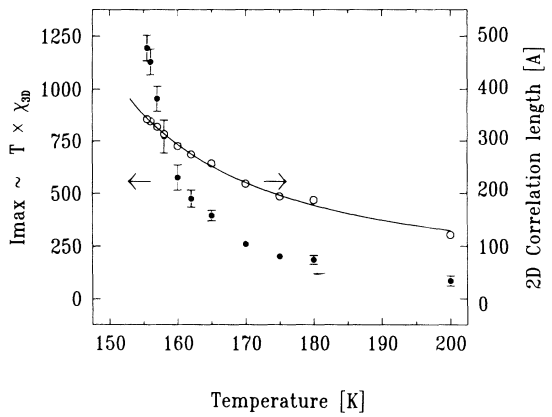

FIG. 4. Temperature dependence of the maximum intensity of the diffuse scattering, measured at the critical wave vector (solid circles). The temperature variation of the 2D correlation length (open circles) is deduced from standard analysis of weakly coupled layers. The solid line is a guide for the eye.

at the same scattering vector as $I_D(q)$ we get

$$\lambda = \frac{kT^*}{\langle\Delta\rangle^2} \frac{I_B}{I_D^{\max}} \pi^{3/2} w_1 w_2 w_3 , \quad (6)$$

where $\pi^{3/2} w_1 w_2 w_3$ is the volume of the Gaussian resolution function in reduced units and $\langle\Delta\rangle$ is the order parameter measured at low temperature. Using previous x-ray results[10] which show that the longitudinal component of the distortion wave q_1 is dominated by the displacement of Nb atoms on the yellow chains with an amplitude of about 2%, and using our experimental value of T^* which is about T_1+2 K we find from Eq. (6) that the coupling energy is $\lambda = 30 \pm 5$ K per unit cell. Introducing this value into Eqs. (4) and (5), we readily deduce the temperature dependence of the 2D correlation length $\xi_{2D}(T)$, as shown in Fig. 4.

In conclusion, we have shown the existence of 2D correlations in $NbSe_3$ associated with the q_1 CDW. The system is more adequately described by weakly coupled (a,b) layers which are very likely the slabs formed by the chains with the shortest Se-Se bonding. We have also shown, in contrast to what is published, that the wave vector q_1 has an important temperature dependence well accounted for by activated variation. With respect to the pronounced two dimensionality and activated variation of the wave vector of the q_1 CDW, $NbSe_3$ appears to be very similar to the blue bronzes which exhibit the same variety of nonlinear transport properties associated with the CDW.

The work at Brookhaven National Laboratory is supported by the Division of Material Sciences, U.S. Department of Energy under Contract No. DE-ACO2-CH00016.

---

[a]On leave of absence from Laboratoire de Physique des Solides, Orsay, France.

[1]For review, see *Electronic Properties of Inorganic Quasi-One-Dimensional Compounds,* edited by P. Monceau, Physics and Chemistry of Materials with Low Dimensional Structures, Ser. B (Reidel, Dordrecht, 1985).

[2]K. Tsutsumi *et al.*, Phys. Rev. Lett. **39**, 1675 (1977).

[3]R. M. Fleming, D. E. Moncton, and D. B. McWhan, Phys. Rev. B **18**, 5560 (1978).

[4]N. P. Ong and J. W. Brill, Phys. Rev. B **18**, 5265 (1978).

[5]J. L. Hodeau *et al.*, J. Phys. C **11**, 4117 (1978).

[6]J. A. Wilson, Phys. Rev. B **19**, 6456 (1979); J. Phys. F **12**, 2469 (1982).

[7]J. P. Pouget *et al.*, J. Phys. (Paris) **46**, 1731 (1985).

[8]J. H. Ross, Jr., Z. W. Wang, and C. P. Slichter, Phys. Rev. Lett. **56**, 663 (1986).

[9]D. J. Scalapino, Y. Imry, and P. Pincus, Phys. Rev. B **11**, 2042 (1975).

[10]A. H. Moudden, S. Girault, J. P. Pouget, P. Monceau, and F. Levy (to be published).